scientific reports

Check for updates

OPEN

Dysregulation of REST and its target genes impacts the fate of neural progenitor cells in down syndrome

Tan Huang[1], Sharida Fakurazi[2], Pike-See Cheah[2,3,4] & King-Hwa Ling[1,3,4,5]✉

Increasing shreds of evidence suggest that neurogenic-to-gliogenic shift may be critical to the abnormal neurodevelopment observed in individuals with Down syndrome (DS). REST, the Repressor Element-1 Silencing Transcription factor, regulates the differentiation and development of neural cells. Downregulation of REST may lead to defects in post-differentiation neuronal morphology in the brain of the DS fetal. This study aims to elucidate the role of REST in DS-derived NPCs using bioinformatics analyses and laboratory validations. We identified and validated vital REST-targeted DEGs: CD44, TGFB1, FN1, ITGB1, and COL1A1. Interestingly, these genes are involved in neurogenesis and gliogenesis in DS-derived NPCs. Furthermore, we identified nuclear REST loss and the neuroblast marker, DCX, was downregulated in DS human trisomic induced pluripotent stem cells (hiPSCs)-derived NPCs, whereas the glioblast marker, NFIA, was upregulated. Our findings indicate that the loss of REST is critical in the neurogenic-to-gliogenic shift observed in DS-derived NPCs. REST and its target genes may collectively regulate the NPC phenotype.

Keywords REST, NPC, Down syndrome, Neurogenesis, Gliogenesis

Down syndrome is a genetic condition resulting from the triplication of chromosome 21 (T21), which leads to intellectual disability. It has a prevalence of 1 out of every 800 lives born globally[1]. The DS phenotype may arise due to gene dysregulation on non-chromosome 21 genes, potentially driven by the overexpression of trisomic genes on T21. DS is associated with a range of neurodevelopmental and neurodegenerative changes, including diminished brain size, reduced overall brain weight, structural brain hypoplasia, a lower neuronal count, an increased population of astrocytes, abnormalities in dendritic structure, and Alzheimer's disease (AD)-like symptoms[2,3]. These neural deficits are linked to the impaired function of neural progenitor cells (NPCs), which are multipotent stem cells in the developing brain capable of differentiating into neurons, astrocytes and oligodendrocytes[4]. DS hiPSC-derived NPCs experience a genome-wide chromosomal reorganisation leading to a senescence-like response, including altered chromatin states and gene transcription[5]. DS hiPSC-derived NPCs exhibit aberrant differentiation patterns, characterised by an increased tendency to differentiate into glial cells, especially astrocytes, and a reduced propensity to form neurons[6]. These studies highlight the pivotal role of NPC dysfunction in the pathogenesis of Down syndrome; however, the underlying molecular mechanisms driving NPC impairment in this condition remain poorly understood.

The Repressor Element-1 Silencing Transcription Factor (REST), also known as the Neuronal Restriction Silencing Factor (NRSF), is well-recognized for its regulatory role in controlling gene expression in NPCs and embryonic development[7]. REST is a transcriptional repressor that regulates target genes by binding to repressor element 1 (RE1), the conserved 23 bp DNA motif[8]. During this process, REST recruits cofactors, such as CoREST, N-CoR, and mSin3A, to form a REST-repressor complex that induces changes in chromatin state and nucleosome repositioning[9,10]. A genome-wide analysis has discovered that over 1,892 RE1 binding sites exist in the human genome[11]. The Gene Transcription Regulation Database (GTRD) identifies 15,450 REST

[1]Department of Biomedical Sciences, Faculty of Medicine and Health Sciences, Universiti Putra Malaysia, Serdang 43400, Selangor, Malaysia. [2]Department of Human Anatomy, Faculty of Medicine and Health Sciences, Universiti Putra Malaysia, Serdang 43400, Selangor, Malaysia. [3]Brain and Mental Health Research Advancement and Innovation Networks (PUTRA® BRAIN), Universiti Putra Malaysia, Serdang 43400, Selangor, Malaysia. [4]Malaysian Research Institute on Ageing (MyAgeing®), Universiti Putra Malaysia, Serdang 43400, Selangor, Malaysia. [5]Department of Biomedical Sciences, Faculty of Medicine and Health Sciences, Universiti Putra Malaysia, Serdang 43400, Selangor, Malaysia. ✉email: lkh@upm.edu.my

target genes within the human genome, providing the most extensive collection of consistently processed ChIP-sequencing data for mapping transcription factor binding sites in humans[12]. REST regulates necessary epigenetic modifications in neural development, synaptic function, and vesicle transport, including DNA methylation, hydroxymethylation, and histone modifications[7,8].

REST proteins are maintained at high expression levels in NPCs to regulate cell pluripotency, differentiation and proliferation[13]. As differentiation progresses towards the neuronal lineage, a reduction in REST expression occurs, resulting in the expression of target genes in neurogenesis and neuronal function[9]. This process governs axon elongation, synaptic communication, membrane responsiveness, and the establishment of neuronal identity. Additionally, REST is pivotal in overseeing the development of glial cell lineages, gliogenesis, and the interactions between neurons and glial cells[14]. During NPC differentiation, the appropriate level of REST is crucial for transitioning from neurogenesis to gliogenesis and maintaining the correct neuron-to-glial cell ratio. REST, initially active during fetal brain development, is later reactivated in the nucleus to safeguard neurons from various stressors, preserve cognitive functions, and promote longevity[15]. In a transchromosomal model of DS, REST expression was reduced by 30–60%, a decrease that persists from embryonic stem (ES) cells to the adult brain with trisomy 21 [16]. Despite its known functions, the specific role of REST in DS-derived NPCs remains inadequately understood. Further research is necessary to elucidate how dysregulation of REST affects these cells.

In this study, we explored the effects of trisomy chromosome 21 on NPCs and examined the potential impacts of REST dysregulation. HiPSC-derived NPCs serve as a powerful platform for investigating the neurodevelopmental aspects of DS. We obtained publicly available datasets of DS hiPSC-derived NPCs and conducted a comprehensive transcriptomic analysis associated with REST target genes. Our study demonstrated that REST-targeted DEGs significantly impact cellular functions and pathways in DS hiPSC-derived NPCs, leading to considerable disruptions during development and differentiation. The REST loss and the dysregulation of its target Hub DEGs impact the fate of DS hiPSC-derived NPCs differentiation.

Materials and methods

Acquisition and process of DS hiPSC-derived NPCs datasets

We obtained the sequence datasets of human induced pluripotent stem cell (hiPSC)-derived NPCs from the Gene Expression Omnibus database (GEO, https://www.ncbi.nlm.nih.gov/geo/). The GSE185192 dataset with the Affymetrix GPL18573 platform includes 18 transcriptome samples from one isogenic pair (3 DS samples and 3 controls) and two non-isogenic pairs (6 DS samples and 6 controls). The GSE208625 dataset with the Affymetrix GPL16791 includes six transcriptome samples from one non-isogenic pair (3 DS samples and 3 controls). The GSE185192 was utilised as a training dataset, and the GSE208625 was used as a validation dataset.

Processing of the dataset and identification of differentially expressed genes (DEGs)

We used the Galaxy web-based platform (https://www.usegalaxy.org/) to analyse the Next-Generation Sequencing (NGS) dataset. The *Trim Galore* software (Galaxy Version 0.6.7 + galaxy0) was used to read and trim the FASTQ files. The *FASTQC* software (Galaxy Version 0.74 + galaxy1) was used to test the quality of individual samples. Subsequently, the *HISAT2* software (Galaxy Version 2.2.1 + galaxy1) was employed to align the transcriptome sequences, using the hg38 human reference genome for annotation. The *htseq-count* software (Galaxy Version 2.0.5 + galaxy0) was used to count aligned reads. Lastly, *DESeq2* software (Galaxy Version 2.11.40.8 + galaxy0) was utilised to analyse differential gene expression between DS and control groups. Genes were classified as DEGs with an adjusted p-value < 0.05 and |log2 FC| > 1. The analysis results were visualised with a heatmap and volcano plot created using RStudio software (Version:2023.03.0 + 386).

Gene set enrichment analysis

The gene set enrichment analysis (GSEA) was employed to detect whether Enrichment analyses for Gene Ontology (GO) and Kyoto Encyclopedia of Genes and Genomes (KEGG)[17] pathways enrichment was statistically significant in DS hiPSC-derived NPCs and controls from the GSE185192 training set. We utilised the three packages (*org.Hs.eg.db*, *clusterProfiler* and *enrichplot*) in RStudio software (Version: 2023.03.0 + 386) for GSEA analysis and visualisation. Results with a corrected enrichment score (NES) showing |NES| > 1 and an adj. $p < 0.05$ were deemed significantly different.

REST-targeted DEGs in DS hiPSC-derived NPCs

REST target genes specific to humans were extracted from the Gene Transcription Regulation Database (GTRD, http://gtrd.biouml.org). To visualise the overlap compared these REST-targeted genes with the DEGs from the GSE185192 training dataset, Venn diagrams were generated using the web tool (https://bioinfogp.cnb.csic.es/tools/venny/). The significance of the gene overlap was then evaluated using the hypergeometric probability model, with the human genome as the reference background (http://nemates.org).

Gene ontology and pathway enrichment analysis

GO and KEGG[17] analysis were conducted on DEGs and REST-targeted DEGs with the R package *clusterProfiler*. The significant enrichment results from GO and KEGG with p-values < 0.05 were considered. The *rrvgo* and *simplifyEnrichment* packages perform semantic similarity analysis on the GO analysis results and cluster the results. The *heatmapPlot* and *complexheatmap* packages were used to visualise the enriched GO and KEGG results. All the analyses were performed using RStudio software (Version: 2023.03.0 + 386).

WGCNA network construction and module identification

Weighted Gene Co-expression Network Analysis (WGCNA) is a systematic approach in biology for clustering multiple genes with similar expression patterns, dividing genes into modules based on relevance. The network was constructed and visualized with the *WGCNA* package using RStudio software (Version: 2023.03.0 + 386). This study performed WGCNA on the GSE185192 training set, which consists of 9 DS and 9 corresponding control samples. The network development was performed using a soft-threshold parameter (β). The value of β was selected by identifying the lowest power achieved at a scale-free topological overlap matrices fit value of 0.9. We conducted Pearson correlation analyses to investigate the interrelationships among gene modules and determine the module that exhibits the strongest correlation with DS. Gene significance (GS) and module membership (MM) values were computed, and the genes with GS of more than 0.5 and MM of more than 0.8 were identified as critically associated with the module.

PPI network construction for screening hub genes

The protein-protein interaction (PPI) network was induced using the Search Tool for the Retrieval of Interacting Genes database (STRING, https://string-db.org/)[18] with an interaction score of at least 0.4. To pinpoint hub genes within the overlapping genes of REST-targeted DEGs and core modules of WGCNA, we constructed a modular gene network using Cytoscape software (version 3.9.1)[19]. The "cytoHubba" plugin was utilised to predict and explore significant nodes or hub genes[20]. To identify hub genes, we used ten topological algorithms of "cytoHubba", including Betweenness, Bottleneck, Closeness, EcCentricity, Edge Percolated Component (EPC), Maximum Cluster Centrality (MCC), Maximum Neighbourhood Component (MNC), Radality, and Stress to obtain the top 20 ranked genes, respectively. The overlap of these 10 gene sets was then identified as the hub genes.

Validation of hub genes

To determine whether the levels of hub gene expression varied significantly between DS hiPSC-derived NPCs and controls, we visualised these levels using scatter plots and box-and-line plots for both the training and validation datasets. Real-time quantitative RT-PCR will then be conducted to validate the mRNA expression level of these hub genes.

Cell culture

In this study, we utilized three trisomic iPSC lines (DS2 (WC-24-02-DS-M), DS3 (UWWC1-2DS3), and DS4 (HPS4270)) and three euploid iPSC lines (C2 (WC-24-02-DS-A), C4 (ATCC-DYS0100), and C5 (HPS4272)). These lines included two pairs of isogenic cell lines (DS2 and C2; DS4 and C5) and one pair of non-isogenic cell lines (DS3 and C4). DS2, C2, and DS3 were obtained from the WiCell Research Institute at the University of Wisconsin[21,22], C5 and DS4 were sourced from the RIKEN BioResource Center in Japan[23], and C4 was acquired from the American Type Culture Collection[24]. Detailed information on the cell lines is provided in Supplementary Table 1. HiPSCs were cultured in complete mTeSR™ Plus medium (comprising Basal Medium and 5X Supplement; STEMCELL Technologies, Canada) on Geltrex-coated six-well plates, following the manufacturer's instructions. Upon reaching approximately 80% confluency, the hiPSCs were dissociated with accutase and seeded onto Geltrex-coated six-well plates at a density of 300,000 cells per well in complete mTeSR™ Plus medium supplemented with 5 μM Y27632. For neural induction, hiPSCs at 20% confluency were exposed to a complete Neural Induction Medium (consisting of Neurobasal Medium and Neural Induction Supplement; Gibco, US) for 7 days, with medium changes every two days, following the manufacturer's instructions. The resulting hiPSC-derived NPCs were expanded in Neural Expansion Medium (comprising Neurobasal Medium, AdvancedTM DMEM/F-12, and Neural Induction Supplement; Gibco, US) on a Geltrex-coated 6-well plate, following the manufacturer's instructions. All cells used in this study were NPCs during maintenance.

MTT assay

Cells were dissociated with Accutase, and the cell suspension was adjusted to a concentration of 8,000 cells in 180μL cell suspension per well of a 96-well plate. The plate was incubated at 37 °C with 5% CO2 for 12 h to allow the cells to adhere. After 12 h, an appropriate concentration of the test compound (lithium carbonate[25] or X5050[26]) was added, and the cells were cultured for 24 h. Following this incubation period, the supernatant was carefully removed, and 90μL of fresh medium was added to each well. Subsequently, 10μL of MTT solution was added, and the cells were incubated for another 4 h. Subsequently, the supernatant was discarded, and 110 μL of Formazan solubilisation solution was introduced into each well. The plate was then placed on a shaker and gently agitated for 10 min to ensure complete dissolution of the formazan crystals. Absorbance was subsequently assessed at 490 nm with a microplate reader (Biochrom Asys UVM 340). Blank wells (containing only medium, MTT, and Formazan solubilisation solution) and control wells (containing cells, the same concentration of drug solvent, medium, MTT, and Formazan solubilisation solution) were set up, with four replicates per group.

Immunocytochemistry

The NPCs derived from hiPSCs were seeded onto Geltrex-coated glass coverslips in Neural Expansion Medium, with medium exchange occurring every second day. Subsequently, cells were fixed in 4% paraformaldehyde (PFA), rinsed with phosphate-buffered saline (PBS), permeabilised in a solution containing 0.3% Triton X-100, 10% donkey serum, and PBS, and subjected to overnight staining at 4 °C. The staining involved Nestin, REST, DCX, and NFIA antibodies in a mixture of 10% donkey serum, 0.3% Triton X-100, and PBS. Following PBS washes, secondary antibodies were applied for 2 h at room temperature, followed by nuclear counterstaining with DAPI. Image acquisition was performed using a fluorescence microscope (Olympus, Japan). The fluorescence micrographs were analysed using Fiji (version 2.14.0/1.54f). The primary antibodies used for

Primer	Sequence (5'-3')	Annealing temperature (℃)	Length (bp)
CD44 F	TACCCCAGCAACCCTACTGA	60	20
CD44 R	GGTCCTGTCCTGTCCAAATCT		21
COL1A1 F	AGGGACACAGAGGTTTCAGT	60	20
COL1A1 R	AGCACCATCATTTCCACGAG		20
DCX F	GAAGGGAAACCCATCAGCCA	60	20
DCX R	GAGGTTCCGTTTGCGTCTTG		20
FN1 F	CCGCCGAATGTAGGACAAGA	60	20
FN1 R	CCGAACCTTATGCCTCTGCT		20
HMBS F	GATGTTAGGAGCCCTGTTTGG	60	21
HMBS R	TTACGAGCAGTGATGCCTACC		21
ITGB1 F	GCCAAATGGGACACGCAAGA	60	20
ITGB1R	TTGACCACAGTTGTTACGGC		20
NFIA F	TGAAGTGGAGCCAGGAATGC	60	20
NFIA R	ATGACAGGTCGGTGATGCTG		20
PSMB2 F	GAGGGCAGTGGAACTCCTTAG	60	21
PSMB2 R	GATGTTAGGAGCCCTGTTTGG		21
REST F	GAGAACGCCCATATAAATGTG	60	21
REST F	CACATAACTGCACTGATCAC		20
TGFB1 F	TTGAGGGCTTTCGCCTTAGC	60	20
TGFB1 R	CGGTAGTGAACCCGTTGATG		20

Table 1. Primer sequences. F, Forward Primer; R, Reverse Primer; CD44, CD44 molecule; COL1A1, Collagen type I alpha 1 chain; DCX, Doublecortin; FN1, Fibronectin 1; HMBS, Hydroxymethylbilane synthase; ITGB1, Integrin subunit beta 1; NFIA, Nuclear factor I A; PSMB2, Proteasome 20 S subunit beta 2; REST, RE1 silencing transcription factor; TGFB1, Transforming growth factor beta 1.

immunodetection were as follows: Anti-REST (22242-1-AP; Proteintech, USA; 1:200 dilution), anti-DCX (CSB-PA006576DA0HU; Cusabio, USA; 1:200 dilution), anti-NFIA (E-AB-67569; Elabscience, USA; 1:200 dilution), anti-SOX2 (ab239218, Abcam, USA; 1:200 dilution) and anti-Nestin (MA1-110; Invitrogen, USA; 1:200 dilution). The secondary antibodies used for immunodetection were as follows: donkey anti-rabbit IgG conjugated with Alexa Fluor 488 (A-21206; Invitrogen, USA; 1:1000 dilution) for REST, DCX and NFIA; donkey anti-mouse IgG conjugated with Alexa Fluor 488 (A-21202; Invitrogen USA; 1:1000 dilution) for Nestin; donkey anti-goat IgG H&L with Alexa Fluor 594 (ab150132, Abcam, USA; 1:2000 dilution) for SOX2.

Quantitative real-time PCR

Quantitative real-time PCR will be performed on NPCs, with total RNAs extracted from cells using the GeneAll® Ribospin™ II RNA extraction kit (Cat No. 314 – 150), following the manufacturer's protocol. RNA purity and concentration were measured with a NanoDrop spectrophotometer. Reverse transcription was done using the LunaScript® RT SuperMix kit (New England Biolabs). A total of 1ug RNA was reverse-transcribed in a 20 µL reaction volume. Real-time quantitative RT-PCR was performed on the cDNA using 1x QuantiNova SYBR Green PCR Master Mix from Qiagen, and the analysis was conducted with the LightCycler® 480 Real-Time PCR System (Roche Diagnostics, Australia). Samples were prepared for duplicate assays, with *HMBS* and *PBMS2* as internal controls. The primer sequences utilised for qRT-PCR are listed in Table 1.

Western blot

NPCs were lysed using RIPA buffer (cat. No:89901, Thermo Scientific) supplemented with a 1X proteinase inhibitor and phosphatase inhibitor cocktail. The resulting protein lysate was obtained from the supernatant. We then measured the total protein concentration using the Pierce™ BCA Protein Assay Kit (Thermo Fisher Scientific, USA, Cat. no. 23225). Proteins were transferred to a PVDF membrane using the Trans-Blot Turbo system (Bio-rad Laboratories, Inc., USA) according to standard procedures. The membranes were blocked with 5% non-fat milk in TBST (20 mM Tris, 150 mM NaCl, 0.1% Tween-20) for one hour at room temperature. This was followed by overnight incubation with the primary antibody in 5% non-fat milk in TBST at 4 °C. The next day, the membranes were rinsed three times with TBST and then incubated with species-specific secondary antibodies. The antibodies were diluted in 5% non-fat milk in TBST and incubated at room temperature for one hour. Chemiluminescence visualisation was carried out using the G: BOX gel documentation system (Synoptics Ltd, UK), and the optical densities of the detected bands were analysed using Fiji (version 2.14.0/1.54f). The primary antibodies used for immunodetection are as follows: Anti-REST (22242-1-AP; Proteintech, USA; 1:1000 dilution), anti-DCX (CSB-PA006576DA0HU; Cusabio, USA; 1:1000 dilution), anti-NFIA (E-AB-67569; Elabscience, USA; 1:1000 dilution), and anti-GAPDH (E-AB-40337; Elabscience, USA; 1:4000 dilution).

Statistical analysis

The data are presented as mean ± standard deviation (SD), with all experiments being conducted in triplicate. Statistical analyses were performed using GraphPad Prism 9.0 (version 9.5.0) or RStudio software (version 2023.03.0 + 386). A significance threshold of $P < 0.05$ was applied, and statistical significance is represented as follows: ns, not significant; $^{*}P < 0.05$; $^{**}P < 0.01$; $^{***}P < 0.001$.

Results

Differentially expressed genes and their ontologies

This study analysed the DEGs in DS hiPSC-derived NPCs (GSE185192). 3,106 DEGs were identified in DS-derived NPCs, including 1,544 upregulated and 1,562 downregulated DEGs (Figure SI for volcano plot and heatmap). The GO enrichment analyses from all DEGs in DS-derived NPCs reveal that these genes are enriched for cell differentiation, nerve development, neuron fate commitment, neuron recognition, Wnt signalling pathway, stem cell development, and neural precursor cell proliferation (Fig. 1).

GSEA analysis revealed abnormalities in neural cell differentiation

The results of the GSEA-GO analysis revealed that gene sets associated with biological processes such as cell fate commitment, central nervous system neuron differentiation, negative regulation of gliogenesis, neuron fate commitment, and regulation of neurogenesis were all downregulated in the DS hiPSC-derived NPCs. These GO-related gene sets were significantly enriched with NES < -1, $p < 1e\text{-}10$ and adj. $p < 2.383e\text{-}08$ (Fig. 2A). We then performed GSEA-KEGG analysis, which showed that the JAK-STAT signalling pathway with NES > 1 was upregulated in DS hiPSC-derived NPCs. At the same time, Wnt signalling pathways with NES < -1 were downregulated (Fig. 2B). The Wnt pathway is crucial for NPC proliferation and neurogenesis. The downregulation of the Wnt signalling pathway may result in defects in neuronal maturation or cause NPCs to exit the neurogenesis stage prematurely[27]. However, the upregulation of the JAK-STAT signalling pathway may lead NPCs to favour differentiation into astrocytes[28].

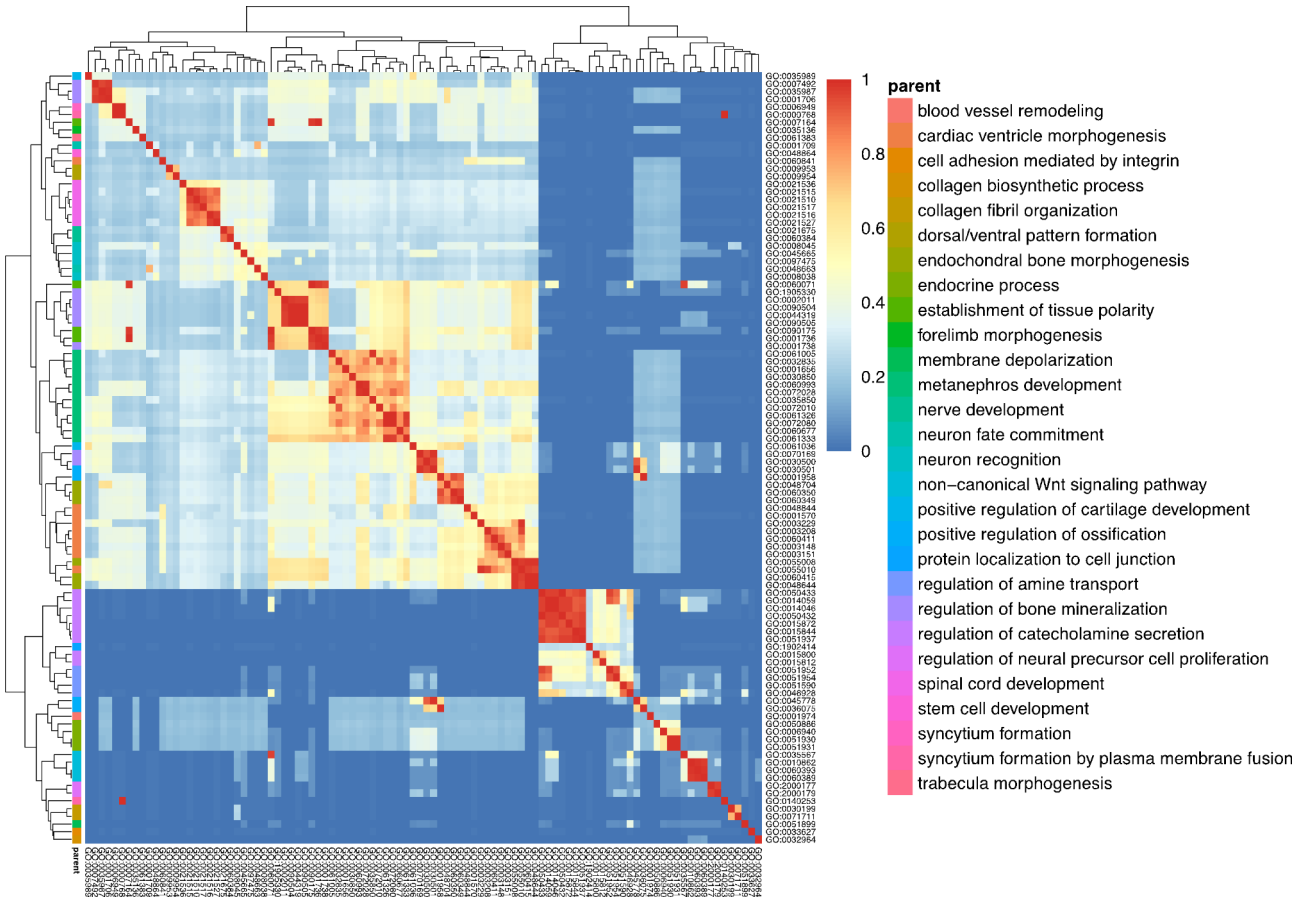

Fig. 1. Biological process clustering enrichment analysis for the DEGs in DS hiPSC-derived NPCs. The top 100 GO terms were clustered based on semantic similarity. The similarity scale ranges from 0 to 1, with colours ranging from blue to red, as indicated by the colour bar. The redder the colour, the closer the similarity value is to 1, indicating higher similarity. GO terms with high semantic similarity are grouped into clusters, as shown by the *parent* bar.

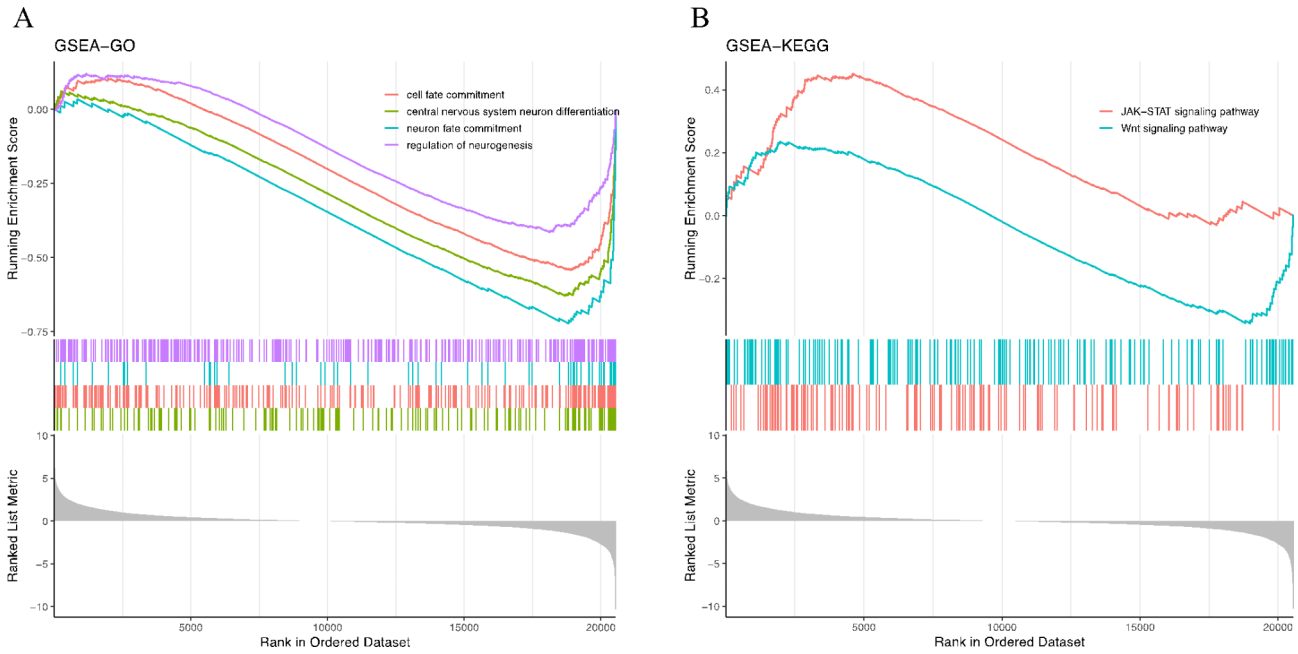

Fig. 2. The GSEA analysis for DS hiPSC-derived NPCs. (**A**) GSEA-GO and (**B**) GSEA-KEGG analysis for the DEGs in DS hiPSC-derived NPCs. All results shown are |NES| >1 and adjusted $p < 0.05$. The graphical representation of the GSEA analysis results is divided into three parts. The top section displays the enrichment score (ES) curves, where different coloured curves represent the ES of gene sets associated with various biological processes and signalling pathways within the ranked gene list (expression matrix). A positive ES indicates that the gene set is enriched at the top of the list, signifying upregulated pathways, while a negative ES indicates enrichment at the bottom, signifying downregulated pathways. The middle section contains coloured bars, each line representing a gene from the corresponding gene set of biological processes and signalling pathways, indicating its position in the ranked gene list. The bottom section shows the distribution of gene expression within the ranked gene list, providing a visual representation of the gene expression levels across the dataset.

REST-targeted DEGs and their ontologies and pathways

To identify DEGs targeted by REST in DS hiPSC-derived NPCs, we compared REST-targeted genes with the DEGs and visualized the results using a Venn diagram (Fig. 3A). We identified 1,965 (63.26%) REST-targeted DEGs in hiPSC-derived NPCs (representation factor, RF = 1.2 and $p < 9.346 \times 10^{-45}$). The GO biological process clustering results reveal that REST-targeted DEGs in hiPSC-derived NPCs are mainly involved in neuron function, cell differentiation, nervous system development, morphogenesis, proliferation, signalling pathway transduction, neurotransmitter secretion and transport, ion concentration, homeostasis, molecular adhesion and metabolism (Fig. 3B). KEGG pathway enrichment analysis indicates the REST-targeted DEGs are involved in the Wnt signalling pathway, TGF-beta signalling pathway, regulating pluripotency of stem cells, MAPK signalling pathway, PI3K-Akt signalling pathway, human papillomavirus infection, focal adhesion and axon guidance (Fig. 3C). The results of GO and KEGG enrichment analysis for genes targeted by REST imply that REST is a critical player in functional regulation and pathological mechanisms for DS hiPSC-derived NPCs.

WGCNA analysis and critical module identification

To identify the critical module associated with DS hiPSC-derived NPCs, we performed WGCNA analysis on all genes from the GSE185192 dataset. Hierarchical clustering of samples was performed based on the distribution of expression values using average chaining and Pearson's correlation to detect outliers (Fig. 4A). The soft threshold power value β is determined to be 13 when the scale-free topology index R^2 initially reaches 0.9, as shown in Fig. 4B. We created a co-expression network using the scale-free topology criteria to detect genes displaying similar expression trends within the same module. In the expression profiles of DS-derived NPCs, eight co-expression modules were identified, each represented by a distinct colour (Fig. 4C). The analysis of module feature correlation revealed that the strongest association with DS-derived NPCs was found in the MEbrown module, comprising 1,278 genes, with a correlation coefficient of 0.73, as illustrated in Fig. 4D. Therefore, 1,278 genes in the MEbrown module were considered as DS-related genes. REST-targeted DEGs were compared with MEbrown module genes to further screen essential genes in REST-targeted DEGs, and 507 overlapping genes (RF = 6.1 and $p < 3.036 \times 10^{-276}$) were obtained for subsequent analysis (Fig. 4E).

PPI network construction and identification of REST-targeted hub DEGs

To further elucidate the hub genes among the overlapping genes from REST-targeted DEGs and WGCNA MEbrown module genes, we constructed the PPI network using the overlap genes, which included 490 nodes

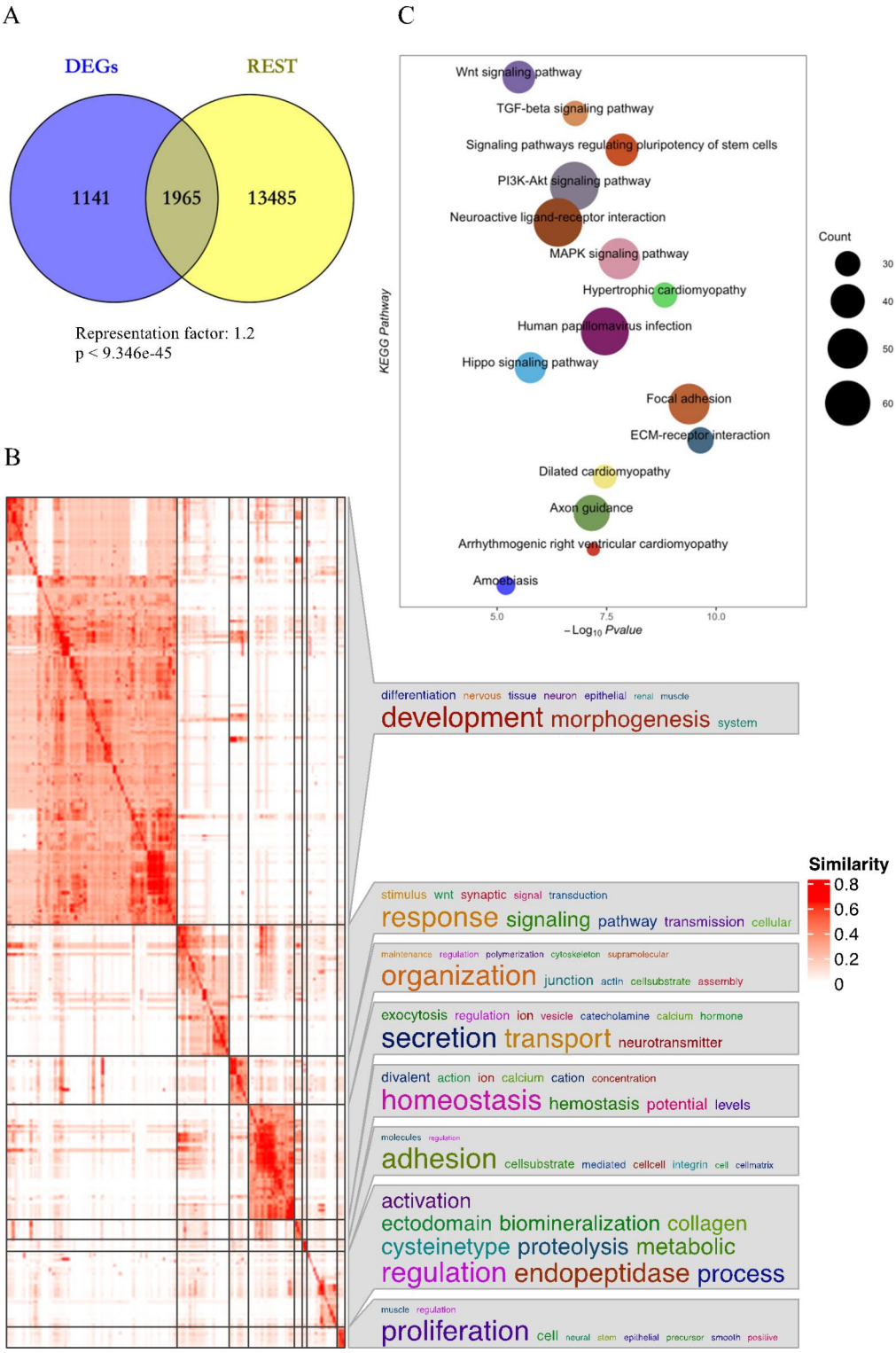

Fig. 3. Enrichment analysis for REST-targeted DEGs. (**A**) The Venn diagram displayed the overlap between REST target genes and DEGs. The overlapping genes are REST-targeted DEGs. (**B**) The top 15 results of KEGG analysis for REST-targeted DEGs in DS hiPSC-derived NPCs were shown. The count refers to the gene numbers enriched in these pathways. The larger the number of genes, the bigger the corresponding circle. (**C**) The biological process clustering enrichment analysis for REST-targeted DEGs in DS hiPSC-derived NPCs. All 1175 GO terms were semantically clustered into 10 categories. On the left is the visualisation of the similarity matrix, where the similarity bar ranges from 0 to 1, indicating the degree of similarity from low to high. Redder colours represent higher similarity values. On the right is the annotation of the clustered GO items in a word cloud.

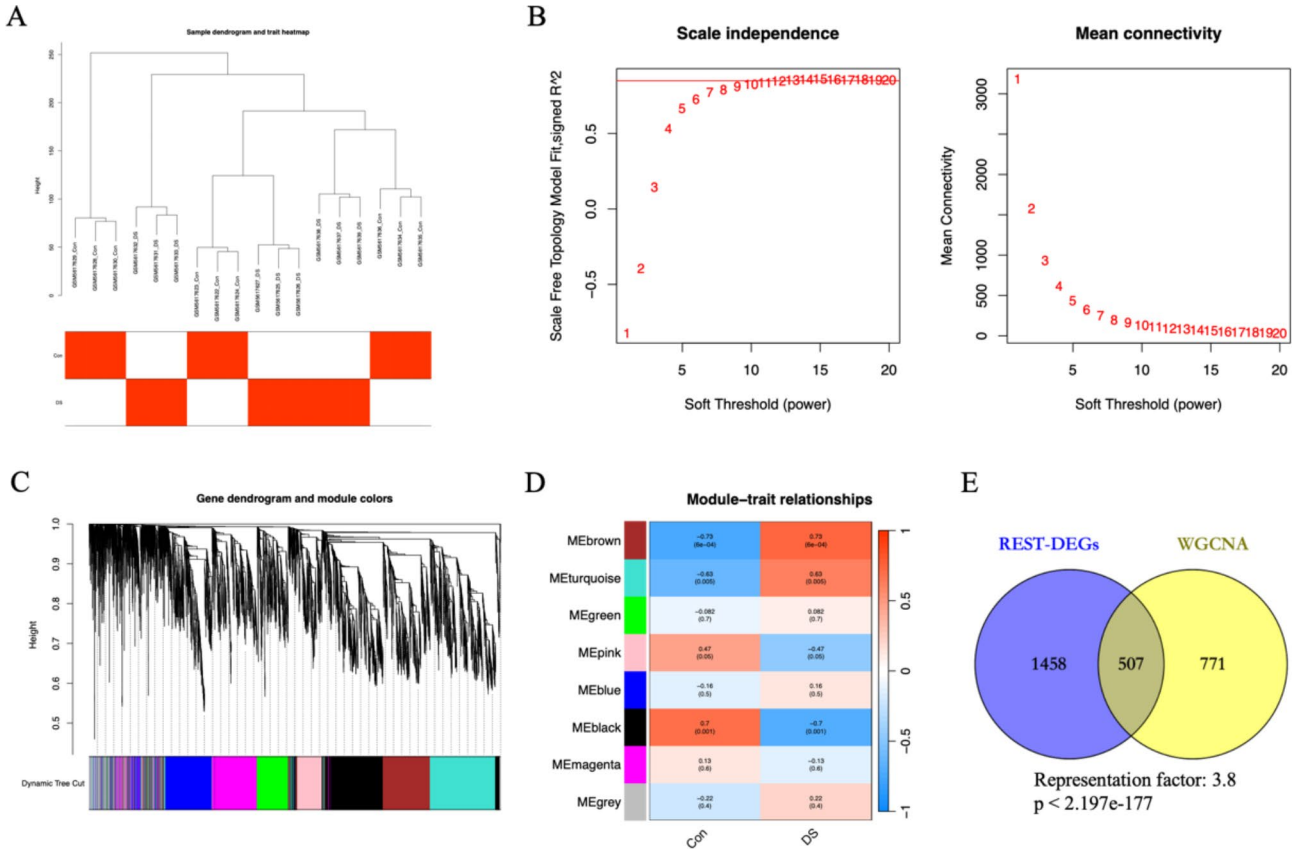

Fig. 4. WGCNA unveiled gene co-expression networks and module-trait relationships. (**A**) Sample clustering was utilized to identify outliers, and a feature heatmap was used to visualize sample characteristics. The network topology was analyzed at different soft threshold powers. (**B**) The graph on the left displays the relationship between the scale-free fit index (y-axis) and the soft threshold powers (x-axis). The graph on the right shows the relationship between mean connectivity (degree, y-axis) and the soft threshold powers (x-axis). A power value (β) of 13 was set for further analysis. (**C**) Clustering dendrograms of all genes based on the topological overlap and assigned module colours was constructed, resulting in 8 distinct co-expression modules represented by different colours. The image displays the relationship between the gene dendrogram at the top and the gene modules at the bottom. (**D**) The analysis examined the relationships between modules and traits. For each module eigengene, the table displays correlations and P-values with different traits. The brown module was identified as the most significantly associated with DS. (**E**) A Venn diagram illustrating the overlap between REST-targeted DEGs and the genes in the brown module.

and 1,495 edges (Figure SII). We then applied 10 different approaches of "cytoHubba" to identify the top 20 most essential genes in the PPI network. Based on the intersection of the top 20 genes through all 10 topological algorithms (Table 2), 6 hub genes were identified, including *CD44*, *TGFB1*, *ALB*, *FN1*, *ITGB1*, and *COL1A1* (Fig. 5). All genes, except for *ALB*, were upregulated in DS hiPSC-derived NPCs. Based on GO analysis of terms (GO:0048863, GO:0051960, GO:0045664, GO:0022604), we found that in addition to *ALB*, the set of genes in which *CD44*, *TGFB1*, *FN1*, *ITGB1*, and *COL1A1* reside are involved in the development and differentiation of NPCs.

In silico and laboratory validation of REST-targeted hub DEGs

To explore the differences in expression levels of the identified hub genes between DS-derived NPCs and controls, we first extracted the expression levels of these genes from the GSE185192 training set. There was a statistically significant difference between the DS hiPSC-derived NPCs and the control group for all the gene expression levels (Fig. 6A). All 6 REST-targeted hub genes except *ALB* were upregulated and involved in the development and differentiation of NPCs. We further validated the expression levels of these genes using a different transcriptomic dataset (GSE208625) derived from the DS hiPSC-derived NPCs. Except for *ALB*, other gene expression levels were significantly upregulated in the DS hiPSC-derived NPCs group compared to the control group (Fig. 6B).

To validate the predicted REST-targeted hub genes, we derived NPCs from 3 controls and DS hiPSCs (Fig. 7A), which pluripotency were confirmed via immunocytochemistry analysis for the OCT4 antigen (Fig. 7B). After 7 days of neural induction in PSC Neural Induction Medium, the hiPSCs differentiated into NPCs. Following one passage, these NPCs were characterised and expanded. Immunocytochemistry showed that NSCs were

MCC	MNC	Degree	EPC	BottleNeck	EcCentricity	Closeness	Radiality	Betweenness	Stress
ALB	*ITGAV*	*ITGAV*	*COL5A2*	*APOB*	*SPARC*	*ELN*	*ELN*	*IRF1*	*EXT1*
CD44	***TGFB2***	*TGFB2*	*COL5A1*	*TLN1*	*ELN*	*ITGA5*	*ITGA5*	*TLN1*	*TLN1*
COL1A1	***FN1***	***FN1***	***FN1***	***ALB***	*CD274*	***FN1***	***FN1***	***FN1***	***CD44***
COL4A1	*AGT*	*SERPINE1*	*TGFB2*	*GNG12*	***ALB***	*AGT*	*AGT*	*FGF10*	*FGF10*
COL5A1	***ITGB1***	***ITGB1***	***ITGB1***	***TGFB1***	*MMP2*	*MMP2*	*MMP2*	***TGFB1***	*TLR4*
COL5A2	*ITGA5*	*ITGA5*	*TIMP2*	*SQSTM1*	***ITGB1***	*SPARC*	*EDN1*	*SPARC*	*SPARC*
COL6A1	*COL6A1*	*COL6A1*	*ITGAV*	*KRT19*	***FN1***	*COL6A1*	*TGFB2*	*SQSTM1*	*GNG12*
ELN	*MMP2*	*MMP2*	***ALB***	*AGT*	*AGT*	*CAV1*	*CAV1*	*CAV1*	*AGT*
FBN1	***COL1A1***	***COL1A1***	*MMP2*	***ITGB1***	*EDN1*	***ITGB1***	***ITGB1***	*AGT*	*CAV1*
FN1	***CD44***	***CD44***	***TGFB1***	*TLR4*	*HBEGF*	***CD44***	***CD44***	***ALB***	***FN1***
ITGA5	*FBN1*	*COL4A2*	*AGT*	*G6PD*	*NRP1*	*EDN1*	*COL6A1*	*MATN2*	*SQSTM1*
ITGAV	*COL4A2*	*SPARC*	*COL4A2*	*TSPO*	*LRP1*	*APOB*	*APOB*	*SERPINE1*	*ITGA5*
ITGB1	*COL5A2*	*COL5A2*	*ELN*	*SPARC*	***CD44***	*FGF10*	*SPARC*	*G6PD*	*MMP2*
MMP2	*TGFB1*	***TGFB1***	***COL1A1***	***CD44***	*IL15*	***TGFB1***	***ALB***	***CD44***	***ALB***
SERPINE1	*CAV1*	*CAV1*	*SERPINE1*	*CAV1*	*APOB*	***COL1A1***	*SERPINE1*	***ITGB1***	***ITGB1***
SPARC	*TLR4*	*TLR4*	*COL6A1*	*SLC16A3*	***TGFB1***	*TLR4*	*TLR4*	*APOB*	*APOB*
TAGLN	*COL4A1*	*COL4A1*	*CAV1*	***COL1A1***	*SERPINE1*	*COL4A1*	*FGF10*	*GNG12*	*SERPINE1*
TGFB1	***ALB***	***ALB***	***CD44***	***FN1***	*TLR4*	***ALB***	***TGFB1***	*TLR4*	***TGFB1***
TGFB2	*SERPINE1*	*AGT*	*COL4A1*	*FGF10*	*FGF10*	*SERPINE1*	***COL1A1***	***COL1A1***	***COL1A1***
TIMP2	*COL5A1*	*COL5A1*	*ITGA5*	*PLAUR*	***COL1A1***	*TGFB2*	*COL4A1*	*EXT1*	*IRF1*

Table 2. The top 20 genes were screened through 10 topological algorithms of "cytoHubba".

positive for Nestin and SOX2 markers (Fig. 7C). To verify the expression of REST-targeted hub genes, the DS hiPSC-derived NPCs samples were collected for RT-qPCR analysis for *CD44*, *TGFB1*, *FN1*, *ITGB1*, and *COL1A1* mRNA expression levels (*ALB* was excluded because no statistically significant differences in mRNA expression levels between DS-derived NPCs and controls in the validation dataset). Our study has shown that the *CD44*, *TGFB1*, *FN1*, *ITGB1*, and *COL1A1* mRNA levels in DS-derived NPCs were significantly upregulated between 1.5 and 2.3 folds in DS compared to the control group (Fig. 7D).

REST loss and neurogenic-to-gliogenic shift in DS hiPSC-derived NPCs

The expression of REST-targeted hub genes (*CD44*, *TGFB1*, *FN1*, *ITGB1* and *COL1A1*) was upregulated in DS-derived NPCs. To further elucidate the role of REST in DS hiPSC-derived NPCs, we conducted Western blot and RT-qPCR on REST. We examined the total REST protein in NPCs, with Western blot results showing a significant reduction in REST protein in DS NPCs compared to the control group (Fig. 8A, B). REST mRNA was significantly downregulated in DS hiPSC-derived NPCs compared to controls (Fig. 8C).

Numerous studies have shown that REST and its target genes *CD44*, *TGFB1*, *FN1*, *ITGB1*, and *COL1A1* regulate NPC proliferation, neurogenesis, and gliogenesis[7,16,29–35]. Although the loss of nuclear REST protein and the dysregulation of REST-targeted hub genes in DS NPCs may disrupt their differentiation, the exact fate of DS NPCs remains unclear. To investigate their effect on the fate of DS-derived NPCs, we measured the DCX (a neuroblast marker) and NFIA (a glioblast marker) expression levels in NPCs. Interestingly, RT-qPCR and Western blot results consistently showed that DCX (Fig. 8A, D, E) was significantly downregulated in DS NPCs compared to the control group. Conversely, RT-qPCR (Fig. 8G) showed that NFIA mRNA was significantly upregulated in DS NPCs. Although Western blot results did not show a significant difference in NFIA protein expression between DS NPCs and the control group, an upward trend was observed in DS NPCs (Fig. 8A, F), possibly due to variations among different cell lines. This suggests that losing nuclear REST may lead NPCs to differentiate into glial cells rather than neurons.

GSEA analysis reveals that the JAK-STAT signalling pathway is significantly upregulated in DS hiPSC-derived NPCs. Our previous study demonstrated that the REST targets the JAK-STAT signalling pathway in DS-derived multiple brain tissues and neural cells[36]. Given that the JAK2-STAT3 signalling pathway activation is crucial for shifting NPC fate from neurons to glial cells in the central nervous system[37], we further examined the mRNA expression levels of *JAK2* and *STAT3* in control and DS hiPSC-derived NPCs. We found that JAK2 and STAT3 were upregulated 7.12-fold and 5.21-fold, respectively, in DS NPCs compared to controls (Fig. 8H, I). It provides additional evidence that the loss of REST may be a critical factor in the neurogenic-to-gliogenic shift in NPCs.

Restoration of nucleus REST inhibits neurogenic-to-gliogenic shift

To further explore the effects of REST loss and its restoration on the fate of DS hiPSC-derived NPCs, these cells were treated with lithium carbonate to restore nuclear REST protein levels[25]. An MTT assay was employed to assess the impact of different concentrations of lithium carbonate on the viability of DS hiPSC-derived NPCs over 24 h. The results indicated that treatment with 5 mM lithium carbonate yielded the best relative viability for DS hiPSC-derived NPCs (Fig. 9A). Additionally, we assessed the impact of 24-hour treatment with X5050,

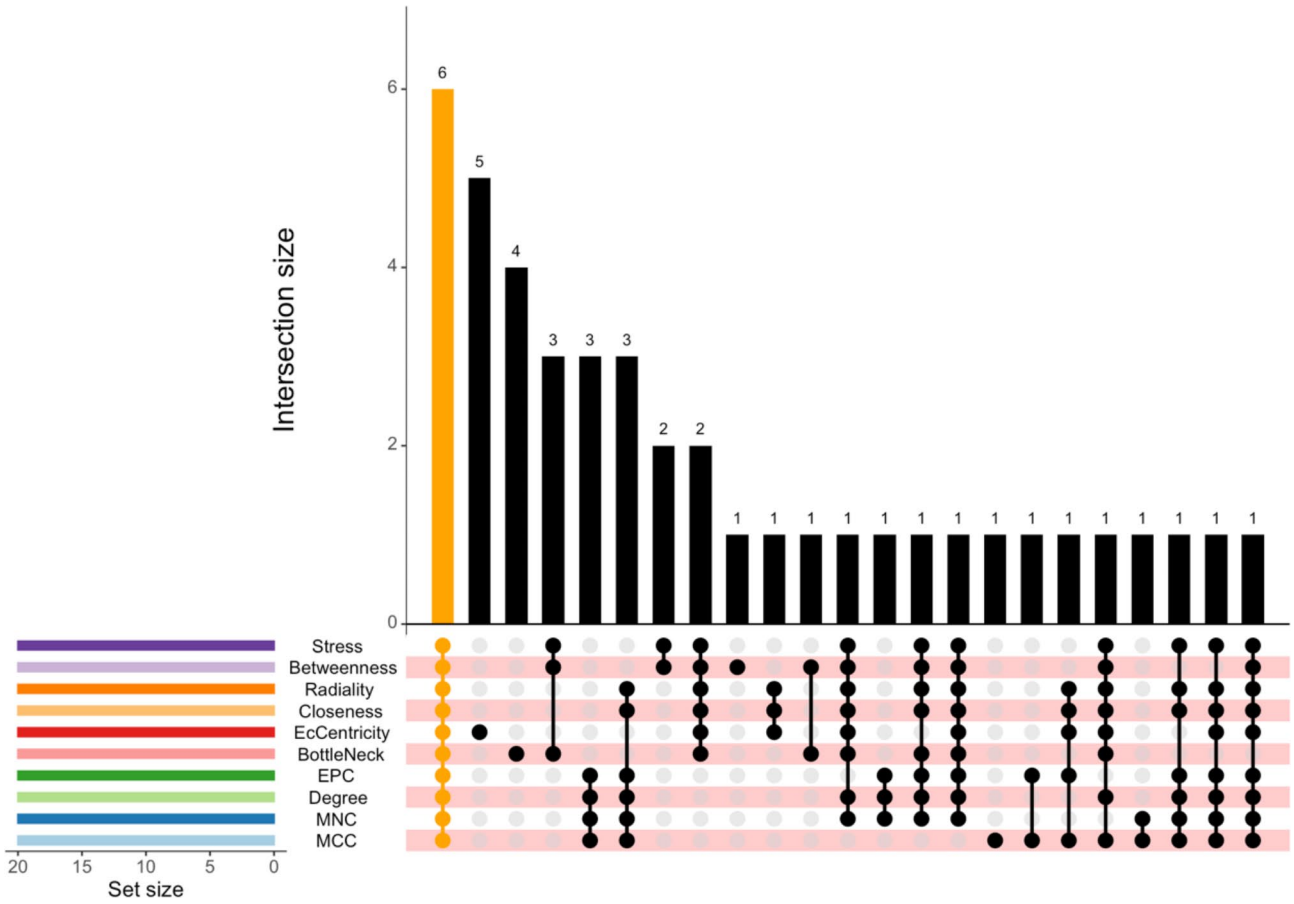

Fig. 5. The UpSet graph provides a comprehensive view of the relationships between the 10 sets, with 6 overlapping genes (*CD44*, *TGFB1*, *ALB*, *FN1*, *ITGB1*, and *COL1A1*). Vertical bars represent the number of genes in the corresponding intersection, while dots with lines represent genes shared between sets. EPC, Edge Percolated Component; MCC, Maximal Clique Centrality; MNC, Maximum Neighborhood Component.

a compound that degrades REST protein[26], on the viability of NPCs. The results showed that 100μM was the optimal concentration for X5050 treatment of DS hiPSC-derived astrocytes over 24 h (Fig. 9B).

Given that REST is a transcription factor, we analysed changes in nuclear REST, DCX and NFIA protein in NPCs by ICC. The ICC results indicated a significant reduction in nucleus REST in DS-derived NPCs (Fig. 9C, D). The DCX was significantly downregulated in DS-derived NPC, while the NFIA was significantly upregulated compared with controls (Fig. 9C, E, F). We further examined the impact of nuclear REST level fluctuations on the expression of DCX and NFIA. Treatment of disomic NPCs with X5050 (Con + X5050 group) significantly reduced nuclear REST expression, which was accompanied by notable downregulation of DCX and upregulation of NFIA compared to controls (Fig. 9C, D-F). Conversely, lithium treatment of trisomic NPCs (DS + Li group) restored nuclear REST expression, resulting in a marked increase in DCX expression and a corresponding decrease in NFIA levels (Fig. 9C, D-F). To validate that these effects were driven by nuclear REST restoration, trisomic NPCs were co-treated with X5050 and lithium (DS + Li + X5050 group). Compared to the Con + Li group, DCX expression was again suppressed, while NFIA expression was significantly elevated (Fig. 9C, D-F). These findings indicate that nuclear REST levels are a critical regulator of DCX and NFIA expression in DS-derived NPCs, potentially reflecting disruptions in transcriptional regulatory pathways mediated by REST.

Discussion

This study explores the role of REST and its target genes in NPCs derived from DS individuals. DS is characterised by severe developmental and functional deficits in the brain, marked by an increase in the number of glial cells and a decrease in neurons. Studies have consistently shown a neurogenic-to-gliogenic shift in DS brains during development, leading to enhanced astrocyte differentiation and functional abnormalities and impaired neuronal cell maturation[38,39]. Genome-wide transcriptional dysregulation in DS-derived NPCs disrupts their ordered differentiation, resulting in abnormal fate determination with increased glial cell differentiation and decreased neuronal differentiation[4]. Previous research underscores the critical role of REST levels in NPCs for maintaining their function. The timely down-regulation or up-regulation of REST serves as a vital switch governing the differentiation of NPCs into neurons and glial cells. Recently, we reported reduced REST expression in neural progenitor cells, adult cortex, and impaired REST nuclear translocation in the prefrontal cortex of the Ts1Cje

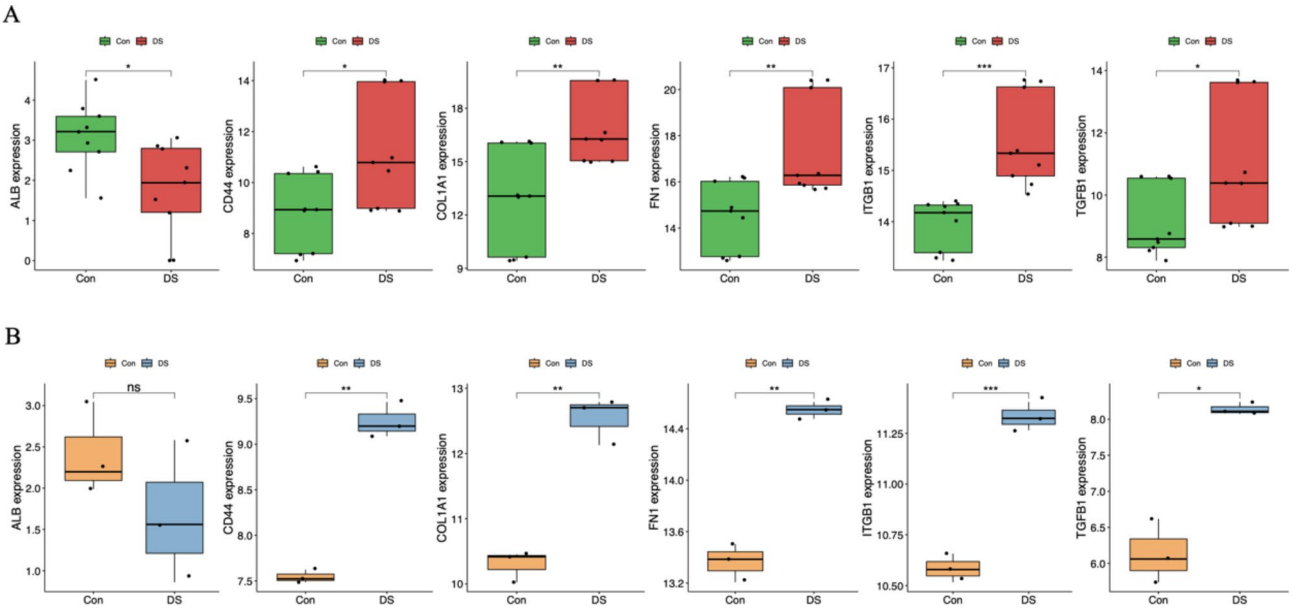

Fig. 6. Validation of REST-targeted hub DEGs at the level of gene expression. (**A**) The expression levels of the 6 REST-targeted hub genes of the GSE185192 training dataset. (**B**) The expression levels of the 6 REST-target hub genes of the GSE208625 validation dataset. The group comparisons were made using the t-test, with a p-value < 0.05 considered as statistically significant. *$P < 0.05$, **$P < 0.01$, ***$P < 0.001$. ns, no significance; Con, Control; DS, Down syndrome.

mouse model of Down syndrome[40]. In the present study, upon REST knockdown in disomic NPCs, we observed changes consistent with those in DS iPSC-derived NPCs, a marked downregulation of DCX and an upregulation of NFIA. Restoration of nuclear REST in DS iPSC-derived NPCs significantly resulted in a significant increase in DCX expression and concurrent suppression of NFIA. These findings suggest that the loss of nuclear REST in NPCs is likely a critical driver of aberrant downstream gene expression and impaired regulation of NPC fate.

We identified and validated five REST-targeted hub genes- *CD44*, *TGFB1*, *FN1*, *ITGB1*, and *COL1A1*-upregulated in DS iPSC-derived NPCs. All five pivotal REST target genes were found to be intricately linked with the regulation of gliogenesis and neurogenesis. CD44 is the cell surface receptor for hyaluronan, an extracellular matrix (ECM) component. Previous research has shown that glial cells, especially astrocytes, are the significant source of CD44 protein in the human brain[41]. CD44 has been widely expressed in astrocyte precursor cells (APCs), and its expression has also been observed in NPCs and oligodendrocyte precursor cells (OPCs)[29]. CD44 deficiency inhibits neural stem cell (NSC) proliferation, leading to delayed neuronal differentiation[30]. Previous studies have also found that CD44 expression is upregulated in transcriptomic data from the brain tissue in DS individuals[42]. Overexpression of CD44 triggers NSCs to differentiate into astrocyte lineage, resulting in greater GFAP expression and increased astrocytes[43]. The upregulation of CD44 in DS-derived NPCs may, therefore, be a critical factor in promoting the differentiation of NPCs into astrocytes.

TGF-β1, a member of the TGF-β family, is involved in neurogenesis, neuronal migration and gliogenesis[28]. A previous study has shown that TGF-β1 treatment reduces neurogenesis and induces premature gliogenesis in both in vitro and in vivo models of mice[31]; however, another study has shown that in vitro hiPSC-derived neural models, TGF-β1 treatment not only increased gliogenesis but also promoted neurogenesis[32]. TGF-β1 is thought to be a potent inducer of the transition of NPCs from neurogenic-to-gliogenic differentiation. During neurodevelopment, NPCs differentiate into the radial glial cell (RG) stage, the starting point for neurons and glial cells. TGF-β1 reduces the pool of Nestin-positive RG cells through activation of the Smad2/3 and MAPK/PPI3K signalling pathways and induces an increase in the expression of GFAP in the somatic cells, which activates signals for gliogenesis[31,44]. Through direct binding of Smad3 to STAT3, TGFβ also cross-talks with JAK-STAT signalling to regulate stem cell self-renewal and differentiation[45]. Interestingly, the GFAP gene promoter activation for astrocytogenesis was observed in cortical neurons by inducing TGF-β1 secretion in a mouse model[46]. Thus, the role of TGF-β1 in NPCs is a critical mechanism in regulating neurogenesis and gliogenesis.

Fibronectin 1 (FN1) is an ECM protein that regulates cell adhesion, migration, proliferation and differentiation[30]. Cell adhesion and migration play an essential role in regulating NSC function. A previous study showed that cell-to-cell contact and cell-ECM adhesion actively promote NSC self-renewal and NSC fate determination by placing stem cells in the vicinity of different signalling signals[47]. A study by Oria et al. showed that FN1 plays a critical role in the differentiation of NPCs into astrocytes and regulates astrocyte migration[48]. In addition, it has been demonstrated that FN1 can activate the JAK-STAT signalling pathway through adhesion molecule mediation and phosphorylation of STAT3 [33], which is a crucial pathway for NPC differentiation

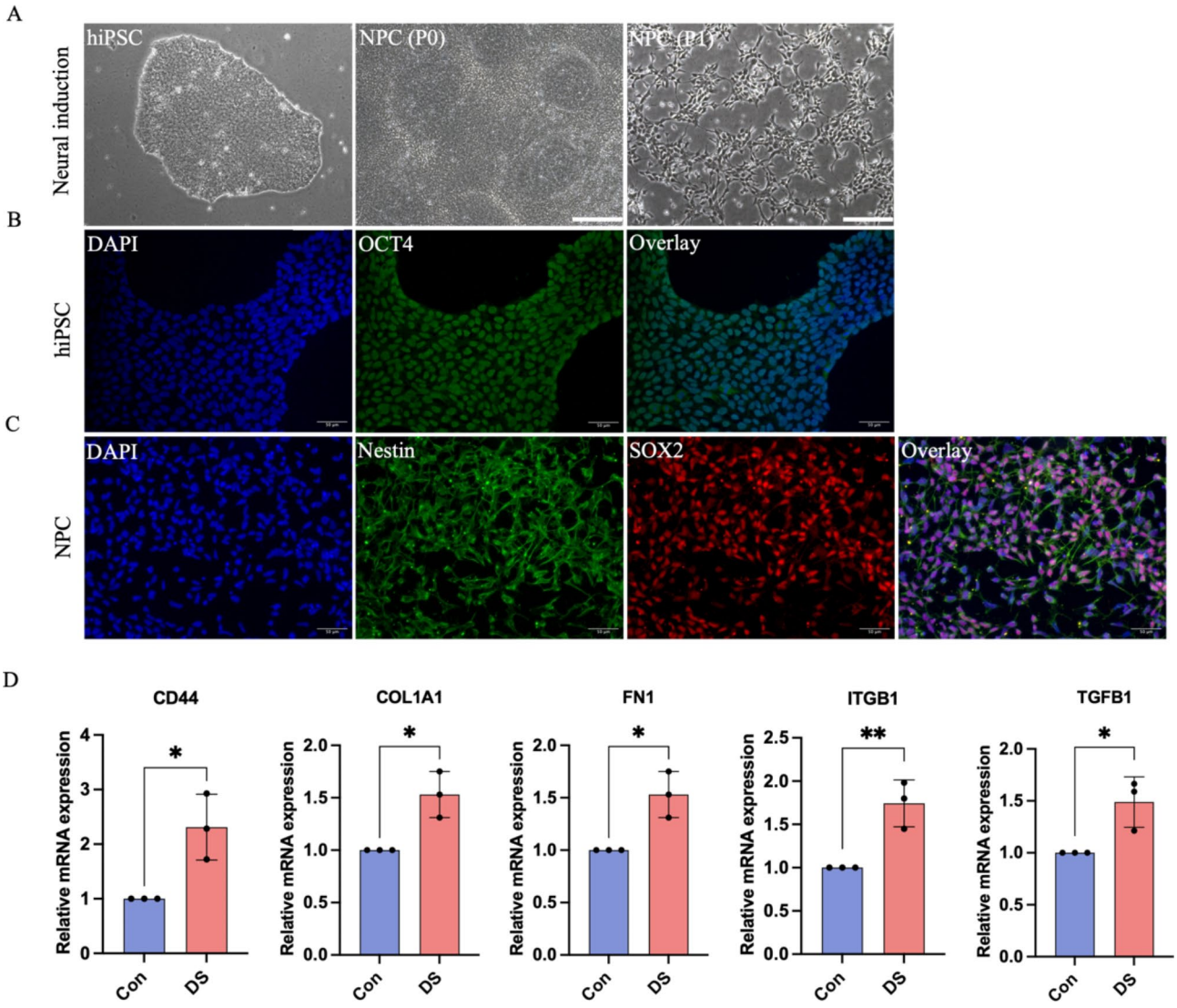

Fig. 7. DS hiPSC-derived NPC cell line establishment and cell characterisation. (**A**) hiPSC undergoing neural induction for 7 days can differentiate into NPC (P0). The stable NPC cell line can be formed after one passaging (P1) (scale bar = 250μm); (**B**) Immunocytochemical staining of hiPSC characteristic cell markers; (**C**) Immunocytochemical staining for NPC characteristic cell markers (scale bar = 50μm); (**D**) The mRNA levels of *CD44*, *TGFB1*, *FN1*, *ITGB1*, and *COL1A1* were detected by RT-qPCR. The mean ± SD is from experiments of three independent cell lines. *$P < 0.05$, **$P < 0.01$. Con, Control; DS, Down syndrome.

and turns on the gliogenic switch[39]. Nevertheless, the precise function of FN1 in NPCs and nervous system development is not yet fully understood.

ITGB1 (β1-integrin) is an integrin family member highly expressed in mammalian embryos and NPCs. ITGB1 is involved in maintaining and differentiating NPCs, cell migration, regulating neurogenesis and gliogenesis, neuronal development, synaptic development and plasticity, and axon formation[34]. Activated ITGB1 crosstalks with the MAPK/PI3K signalling pathway and Wnt/β-catenin signalling pathway to regulate the cell cycle, maintain stem cell properties, and differentiate NSCs[34,49]. ITGB1 regulates the apical adhesion of NSCs during development and promotes their maintenance. Blocking ITGB1 disrupts the NSC microenvironment and tissue architecture[50]. Previous studies have shown that ITGB1 signalling inhibits the differentiation of spinal cord ventricular stem cells and perinatal SVZ NSCs into astrocytes, suggesting that ITGB1 may restrict the fate of NSCs[51,52]. ITGB1 is required for NSC maintenance and neural progeny, and ITGB1 deletion in NSCs results in the rapid loss of NSC identity and differentiation into astrocytes[53]. Transcriptomic and proteomic analyses of the DS hiPSC-derived NPC model revealed increased expression of ITGB1, which was not further investigated[54].

COL1A1 is the gene encoding the α1 chain of type I collagen, a significant component of the ECM of many tissues. The ECM has been shown to play essential roles in neurodevelopmental processes, including neural progenitor cell proliferation, differentiation, morphology, axon and dendritic elongation and connectivity, neuronal migration, and cortical folding[55,56]. The ECM and the ECM receptors (integrin family) have long been known to regulate NPCs behaviour. The binding of ECM to integrins regulates many critical downstream

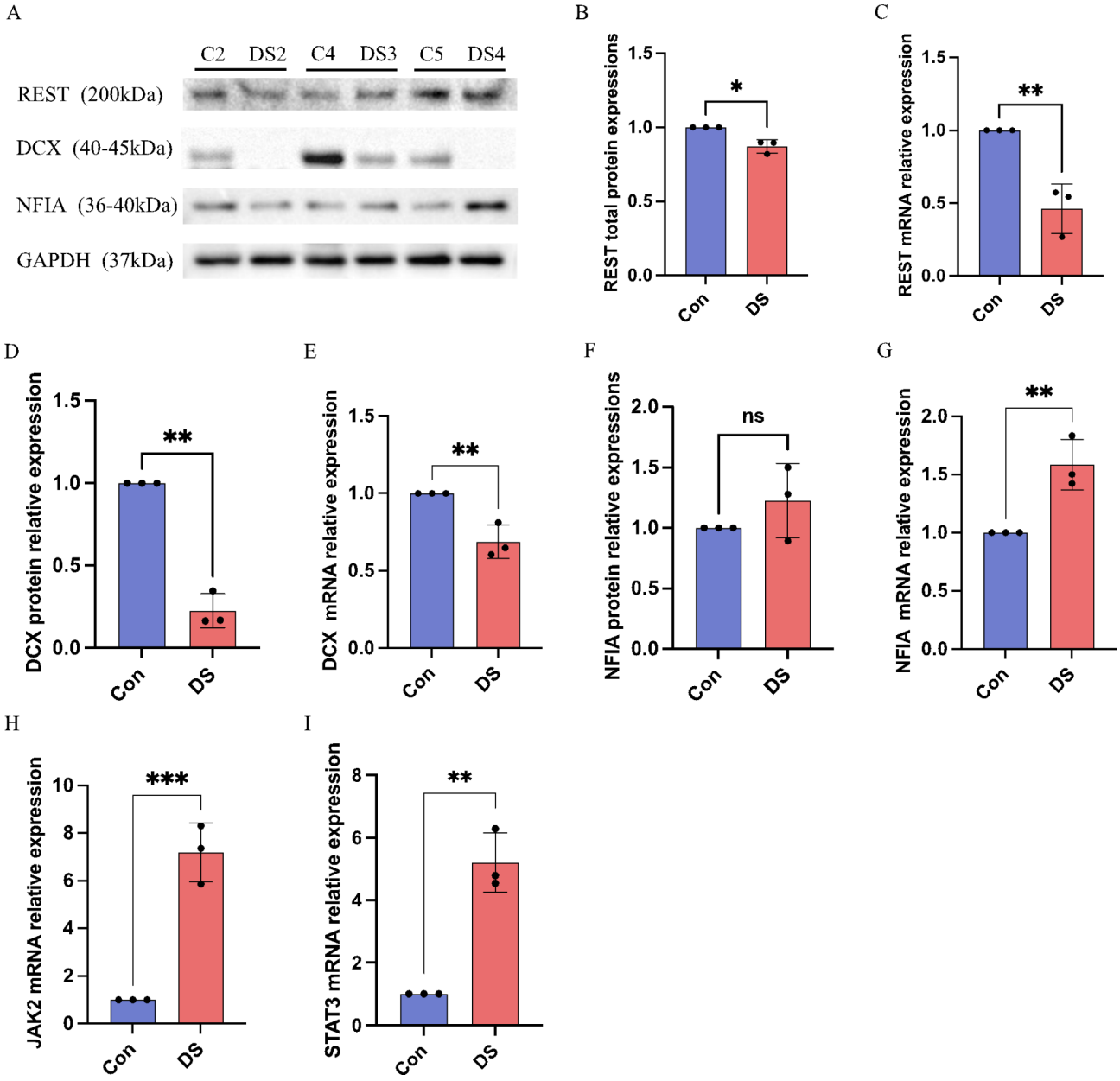

Fig. 8. Three pairs of cell lines (C2 vs. DS2, C4 vs. DS3, and C5 vs. DS4) were used for downstream analyses, including RT-qPCR, and western blot. All measurements were normalised by dividing DS values with their corresponding controls. (**A**) Western blot for the total REST, DCX and NFIA protein in DS-derived NPCs and controls; (**B**-**G**) Protein relative quantitative analysis and RT-qPCR for REST, DCX and NFIA protein and mRNA expressed in DS-derived NPCs and controls; (H, I) RT-qPCR for detection of JAK2 and STAT3 mRNA expressed in DS-derived NPCs and controls, respectively. *$P<0.05$, **$P<0.01$, *** $P<0.001$. Con and C, Control; DS, Down syndrome.

signalling pathways involved in various neurodevelopment aspects, including PI3K-AKT, MAPK, TGF-β, Wnt, and Notch signalling pathways[57,58]. Recently, it has been demonstrated that COL1A1 is a marker for oligodendrocyte precursor cells and that increased expression of COL1A1 may be associated with the generation of oligodendrocyte lineages from NPCs[35]. However, the mechanism by which COL1A1 regulates the differentiation of NPCs into oligodendrocytes remains unclear, and there are few studies of COL1A1 in DS-derived NPCs.

By GSEA analysis, we found that the JAK-STAT signalling pathway was up-regulated in DS iPSC-derived NPCs. Our previous study demonstrated that REST targets the JAK-STAT signalling pathway across human brain tissue and neural cell types in DS[36]. The JAK-STAT pathway is crucial in promoting the switch from neurogenesis to gliogenesis. In this study, we have identified the upregulation of JAK2-STAT3 in DS hiPSC-derived NPCs. STAT3 plays a pivotal role in the self-renewal and differentiation of NPCs. It can be phosphorylated by gp130/

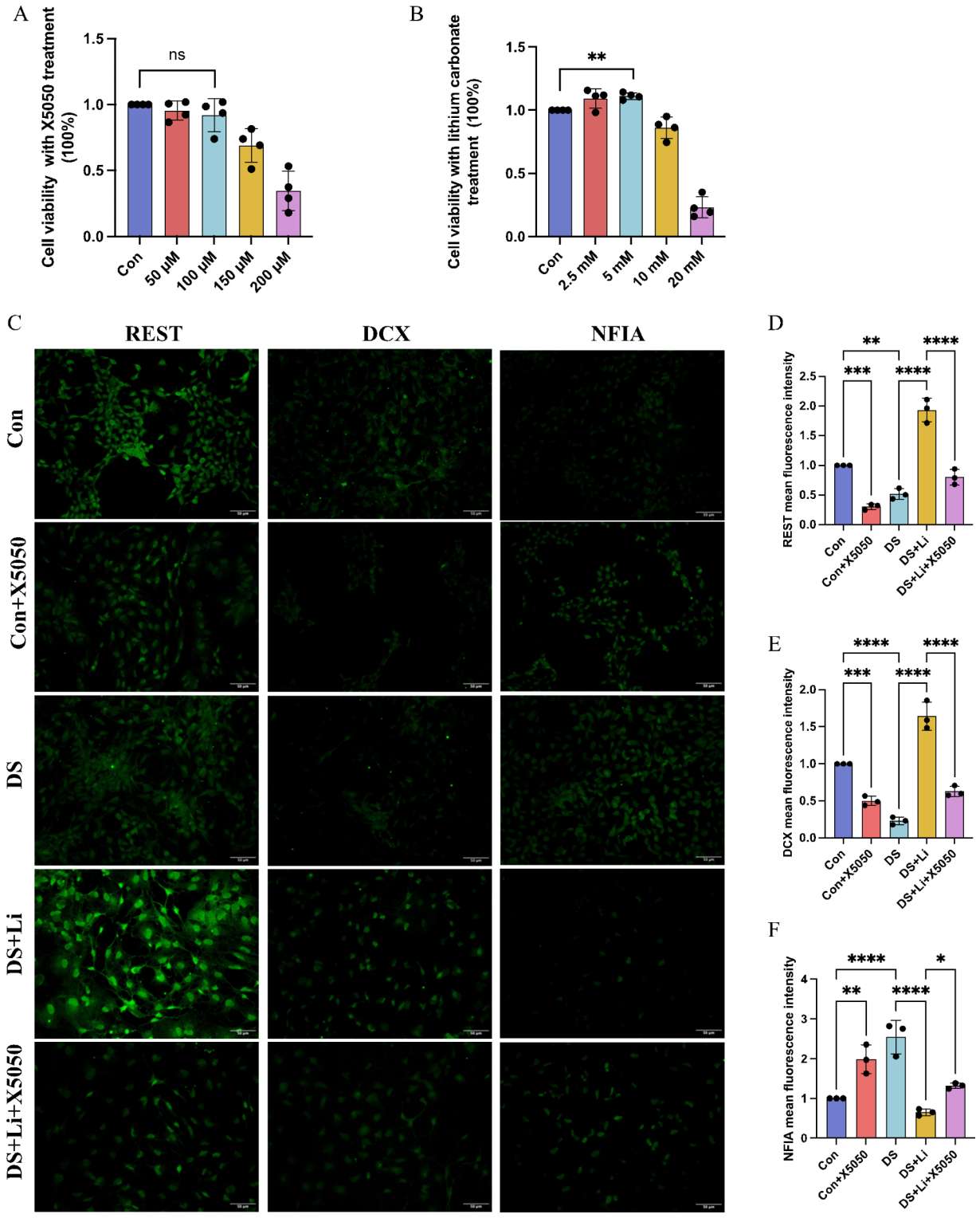

Fig. 9. Three pairs of cell lines (C2 vs. DS2, C4 vs. DS3, and C5 vs. DS4) were used to perform ICC. All cells used in this study were NPCs during maintenance. All measurements were normalised by dividing DS values with the corresponding controls. (**A**, **B**) Optimisation of safety dosage of lithium carbonate and X5050 treatment in iPSC-derived NPCs through MTT cell viability assay. (**C**) ICC validation for REST, DCX and NFIA expressed in the Con group (Control; Disomic NPCs), Con + X5050 group (Disomic NPCs with X5050 treatment), DS + Li group (Trisomic NPCs with lithium carbonate treatment), DS + Li + X5050 (Trisomic NPCs treated with both lithium carbonate and X5050), respectively (scale bar = 50μm); (**D**–**F**) Fluorescence intensity analysis for REST, DCX and NFIA expressed in different groups. *$P < 0.05$, **$P < 0.01$, *** $P < 0.001$, **** $P < 0.0001$. Con and C, Control; DS, Down syndrome.

LIFR-associated JAK1/2 kinases, enabling its translocation to the nucleus and activating the transcription of target genes. STAT3 also promotes gene expression through tyrosine phosphorylation-independent mechanisms[59]. In NPCs, STAT3 is both necessary and sufficient for astrogenesis. Activated STAT3 forms a complex with SMAD1 and p300, which binds to the glial fibrillary acidic protein (GFAP) promoter containing several STAT3 binding sites, inducing its expression[60]. The Notch, BMP, TGF, and JAK/STAT3 signalling pathways, intersecting at STAT3, synergistically promote astrocyte differentiation from NPCs[45,61]. STAT3 activation promotes NPC proliferation and astrogenesis during neurogenesis while negatively regulating neurogenesis[62]. Therefore, REST may influence the fate shift of DS NPC by regulating JAK-STAT signalling pathways.

To determine whether the differentiation of DS-derived NPCs favors neuronal or glial lineages and to clarify the role of REST in this process, we further examined how changes in REST expression levels in NPCs influence the expression of the cellular markers DCX and NFIA. The results revealed that the expression of DCX and NFIA in NPCs is affected by REST expression levels. DCX, a microtubule-associated protein, undergoes transient expression in the early stages of neurogenesis[63]. Its presence in neuronal precursor cells and immature neurons correlates with cell migration and differentiation[63,64]. Widely utilised as a marker for neurogenesis and neuronal migration in both developing and adult brains, DCX contributes to various aspects of early human brain development, including neurogenesis, neuronal plasticity, axon growth, and synaptogenesis[65]. Maintenance of optimal DCX expression in NPCs is a reliable indicator of neurogenic capability[66]. Disruptions such as knockout and knockdown/reduced DCX expression are linked to impaired neurogenesis, developmental disorders, compromised neuronal migration, and neuronal death, highlighting the multifaceted role of DCX in neurogenesis[64].

In contrast, NFIA is pivotal in neural progenitor and genesis of glial cells. Its necessity and sufficiency for embryonic glial cell generation involve regulating genes crucial for astrocyte migration and maturation[67]. The NF1A transcription factor binds to the GFAP gene promoter, an astrocyte-specific protein, leading to the demethylation of GFAP[68]. Designated as a switch for gliogenesis, NFIA efficiently directs the rapid derivation of functional human astrocytes from pluripotent stem cells[69]. NFIA orchestrates neurogenesis inhibition by inducing the Notch effector Hes5[69] while promoting gliogenesis by suppressing the Notch effector Hes1[70]. In conclusion, the critical role of NFIA in regulating gliogenesis and neurogenesis within neural progenitor cells is underscored by its interactions with various transcription factors and signalling pathways, which are crucial for the normal development and differentiation of neural cells. This suggests that the dysregulation of REST may be a key factor for the DS-derived NPCs favouring glial cell lineage differentiation.

Conclusion

REST is a transcriptional repressor that regulates the proliferation and differentiation of neural stem cells. However, few studies have explored the role of REST and its target genes in DS-derived NPCs. This study revealed that REST and its target genes play crucial roles in the proliferation, differentiation, and development of DS-derived NPCs. We propose that the loss of REST is critical in the neurogenic-to-gliogenic shift observed in DS-derived NPCs and that REST and its target genes may collectively regulate the NPC phenotype. However, further research is required to investigate the specific molecular mechanisms and pathways through which the loss of nuclear REST in DS-derived NPCs disrupts their fate.

Data availability

All sequencing data analysed in this study can be found in the original published articles in the GEO database. All experimental data generated during this study are included in this published article.

Received: 19 September 2024; Accepted: 17 January 2025
Published online: 22 January 2025

References

1. Bull, M. J. Down syndrome *N Engl. J. Med.* **382**, 2344–2352 (2020).
2. Antonarakis, S. E. Down syndrome and the complexity of genome dosage imbalance. *Nat. Rev. Genet.* **18**, 147–163 (2017).
3. Antonarakis, S. E., Lyle, R., Dermitzakis, E. T., Reymond, A. & Deutsch, S. Chromosome 21 and Down syndrome: From genomics to pathophysiology. *Nat. Rev. Genet.* **5**, 725–738 (2004).
4. Stagni, F., Giacomini, A., Emili, M., Guidi, S. & Bartesaghi, R. Neurogenesis impairment: An early developmental defect in Down syndrome. *Free Radic. Biol. Med.* **114**, 15–32 (2018).
5. Letourneau, A. et al. Domains of genome-wide gene expression dysregulation in Down's syndrome. *Nature* **508**, 345–350 (2014).
6. Meharena, H. S. et al. Down-syndrome-induced senescence disrupts the nuclear architecture of neural progenitors. *Cell. Stem Cell.* **29**, 116–130e7 (2022).
7. Ballas, N., Grunseich, C., Lu, D. D., Speh, J. C. & Mandel, G. REST and its corepressors mediate plasticity of neuronal gene chromatin throughout neurogenesis. *Cell* **121**, 645–657 (2005).
8. Thiel, G., Ekici, M. & Rössler, O. G. RE-1 silencing transcription factor (REST): A regulator of neuronal development and neuronal/endocrine function. *Cell. Tissue Res.* **359**, 99–109 (2015).
9. Baldelli, P. & Meldolesi, J. The transcription Repressor REST in adult neurons: Physiology, Pathology, and diseases. *eNeuro* **2**, ENEURO0010–152015 (2015).
10. Huang, Y., Myers, S. J. & Dingledine, R. Transcriptional repression by REST: Recruitment of Sin3A and histone deacetylase to neuronal genes. *Nat. Neurosci.* **2**, 867–872 (1999).
11. Sun, Y. M. et al. Distinct profiles of REST interactions with its target genes at different stages of neuronal development. *MBoC* **16**, 5630–5638 (2005).
12. Kolmykov, S. et al. GTRD: An integrated view of transcription regulation. *Nucleic Acids Res.* **49**, D104–D111 (2021).
13. Johnson, R. et al. REST regulates distinct transcriptional networks in embryonic and neural stem cells. *PLoS Biol.* **6**, e256 (2008).
14. Pajarillo et al. Astrocytic transcription factor REST upregulates glutamate transporter EAAT2, protecting dopaminergic neurons from manganese-induced excitotoxicity. *J. Biol. Chem.* **101372** https://doi.org/10.1016/j.jbc.2021.101372 (2021).

15. Lam, X. J., Maniam, S., Cheah, P. S. & Ling K.H. REST in the road map of brain development. *Cell. Mol. Neurobiol.* **43**, 3417–3433 (2023).
16. Canzonetta, C. et al. DYRK1A-Dosage imbalance perturbs NRSF/REST levels, deregulating pluripotency and embryonic stem cell fate in Down Syndrome. *Am. J. Hum. Genet.* **83**, 388–400 (2008).
17. Kanehisa, M. & Goto, S. KEGG: kyoto encyclopedia of genes and genomes. *Nucleic Acids Res.* **28**, 27–30 (2000).
18. Szklarczyk, D. et al. STRING v11: protein-protein association networks with increased coverage, supporting functional discovery in genome-wide experimental datasets. *Nucleic Acids Res.* **47**, D607–D613 (2019).
19. Shannon, P. et al. Cytoscape: A software environment for integrated models of biomolecular interaction networks. *Genome Res.* **13**, 2498–2504 (2003).
20. Chin, C. H. et al. cytoHubba: Identifying hub objects and sub-networks from complex interactome. *BMC Syst. Biol.* **8** (Suppl 4), S11 (2014).
21. Giffin-Rao, Y. et al. Altered patterning of interneuron progenitors in Down syndrome. 02.18.951756 Preprint at (2020). https://doi.org/10.1101/2020.02.18.951756 (2020).
22. Weick, J. P. et al. Deficits in human trisomy 21 iPSCs and neurons. *Proc. Natl. Acad. Sci. U S A.* **110**, 9962–9967 (2013).
23. Wakita, S. et al. Experimental method for haplotype phasing across the entire length of chromosome 21 in trisomy 21 cells using a chromosome elimination technique. *J. Hum. Genet.* **67**, 565–572 (2022).
24. Wren, M. C. et al. Frontotemporal dementia-associated N279K tau mutant disrupts subcellular vesicle trafficking and induces cellular stress in iPSC-derived neural stem cells. *Mol. Neurodegener.* **10**, 46 (2015).
25. Song, Z., Yang, W., Zhou, X., Yang, L. & Zhao, D. Lithium alleviates neurotoxic prion peptide-induced synaptic damage and neuronal death partially by the upregulation of nuclear target REST and the restoration of wnt signaling. *Neuropharmacology* **123**, 332–348 (2017).
26. Charbord, J. et al. High throughput screening for inhibitors of REST in neural derivatives of human embryonic stem cells reveals a chemical compound that promotes expression of neuronal genes. *Stem Cells.* **31**, 1816–1828 (2013).
27. Gulacsi, A. A. & Anderson, S. A. β-catenin–mediated wnt signaling regulates neurogenesis in the ventral telencephalon. *Nat. Neurosci.* **11**, 1383–1391 (2008).
28. He, F. et al. A positive autoregulatory loop of Jak-STAT signaling controls the onset of astrogliogenesis. *Nat. Neurosci.* **8**, 616–625 (2005).
29. Naruse, M., Shibasaki, K., Yokoyama, S., Kurachi, M. & Ishizaki, Y. Dynamic changes of CD44 expression from progenitors to subpopulations of astrocytes and neurons in developing Cerebellum. *PLoS One.* **8**, e53109 (2013).
30. Su, W. et al. CD44 transmembrane receptor and Hyaluronan regulate adult hippocampal neural stem cell quiescence and differentiation. *J. Biol. Chem.* **292**, 4434–4445 (2017).
31. Stipursky, J. et al. TGF-β1 promotes cerebral cortex radial glia-astrocyte differentiation in vivo. *Front. Cell. Neurosci.* **8**, 393 (2014).
32. Izsak, J. et al. TGF-β1 suppresses proliferation and induces differentiation in human iPSC neural in vitro models. *Front. Cell. Dev. Biol.* **8**, 571332 (2020).
33. Song, J. et al. PTPRM methylation induced by FN1 promotes the development of glioblastoma by activating STAT3 signalling. *Pharm. Biol.* **59**, 902–909 (2021).
34. Chang, R. et al. ITGB1-DT facilitates Lung Adenocarcinoma Progression via forming a positive feedback Loop with ITGB1/Wnt/β-Catenin/MYC. *Front. Cell. Dev. Biology.* **9**, 631259 (2021).
35. Marques, S. et al. Transcriptional convergence of Oligodendrocyte lineage progenitors during development. *Dev. Cell.* **46**, 504–517e7 (2018).
36. Huang, T., Fakurazi, S., Cheah, P. S. & Ling, K. H. REST targets JAK–STAT and HIF-1 signaling pathways in human down syndrome brain and neural cells. *IJMS* **24**, 9980 (2023).
37. Kong, X. et al. JAK2/STAT3 signaling mediates IL-6-inhibited neurogenesis of neural stem cells through DNA demethylation/methylation. *Brain Behav. Immun.* **79**, 159–173 (2019).
38. Kawatani, K. et al. A human isogenic iPSC-derived cell line panel identifies major regulators of aberrant astrocyte proliferation in Down syndrome. *Commun. Biol.* **4**, 1–15 (2021).
39. Lee, H. C., Tan, K. L., Cheah, P. S. & Ling, K. H. Potential Role of JAK-STAT Signaling Pathway in the Neurogenic-to-Gliogenic Shift in Down Syndrome Brain. *Neural Plast* 7434191 (2016). (2016).
40. Chong-Teik et al. Reduced REST expression in neural progenitor cells, Adult Cortex, and impaired REST Nuclear translocation in the Prefrontal cortex of Ts1Cje mouse model of Down Syndrome. *Neurochem J.* **18**, 147–161 (2024).
41. Girgrah, N. et al. Localization of the CD44 glycoprotein to fibrous astrocytes in normal white matter and to reactive astrocytes in active lesions in multiple sclerosis. *J. Neuropathol. Exp. Neurol.* **50**, 779–792 (1991).
42. Zamanian Azodi, M., Rezaei Tavirani, M., Rezaei Tavirani, M. & Rostami Nejad, M. Bioinformatics Investigation and Contribution of other chromosomes besides chromosome 21 in the risk of Down Syndrome Development. *Basic. Clin. Neurosci.* **12**, 79–88 (2021).
43. Liu, Y. et al. CD44 expression identifies astrocyte-restricted precursor cells. *Dev. Biol.* **276**, 31–46 (2004).
44. Stipursky, J., Francis, D. & Gomes, F. C. A. Activation of MAPK/PI3K/SMAD pathways by TGF-β1 controls differentiation of radial glia into astrocytes in vitro. *Dev. Neurosci.* **34**, 68–81 (2012).
45. Wang, G. et al. STAT3 selectively interacts with Smad3 to antagonize TGF-β signalling. *Oncogene* **35**, 4388–4398 (2016).
46. de Spohr, S., Martinez, T. C. L., da Silva, R., Neto, E. F., Gomes, F. C. & V. M. & A. neuro-glia interaction effects on GFAP gene: A novel role for transforming growth factor-beta1. *Eur. J. Neurosci.* **16**, 2059–2069 (2002).
47. Morante-Redolat, J. M. & Porlan, E. Neural stem cell regulation by adhesion molecules within the subependymal niche. *Front. Cell. Dev. Biol.* **7**, 102 (2019).
48. Oria, M. et al. Premature neural progenitor cell differentiation into astrocytes in retinoic acid-induced spina bifida rat model. *Front. Mol. Neurosci.* **15**, 888351 (2022).
49. Campos, L. S. et al. Beta1 integrins activate a MAPK signalling pathway in neural stem cells that contributes to their maintenance. *Development* **131**, 3433–3444 (2004).
50. Kazanis, I. et al. Quiescence and activation of stem and precursor cell populations in the subependymal zone of the mammalian brain are associated with distinct cellular and extracellular matrix signals. *J. Neurosci.* **30**, 9771–9781 (2010).
51. North, H. A., Pan, L., McGuire, T. L., Brooker, S. & Kessler, J. A. β1-Integrin alters ependymal stem cell BMP receptor localization and attenuates astrogliosis after spinal cord injury. *J. Neurosci.* **35**, 3725–3733 (2015).
52. Pan, L. et al. β1-Integrin and integrin linked kinase regulate astrocytic differentiation of neural stem cells. *PLoS One.* **9**, e104335 (2014).
53. Brooker, S. M., Bond, A. M., Peng, C. Y. & Kessler, J. A. β1-Integrin restricts astrocytic differentiation of adult hippocampal neural stem cells. *Glia* **64**, 1235–1251 (2016).
54. Sobol, M. et al. Transcriptome and proteome profiling of neural Induced Pluripotent Stem cells from individuals with Down Syndrome disclose dynamic dysregulations of Key pathways and Cellular functions. *Mol. Neurobiol.* **56**, 7113–7127 (2019).
55. Franco, S. J. & Müller, U. Extracellular matrix functions during neuronal migration and lamination in the mammalian central nervous system. *Dev. Neurobiol.* **71**, 889–900 (2011).
56. Long, K. R. & Huttner, W. B. The role of the Extracellular Matrix in neural progenitor cell proliferation and cortical folding during Human Neocortex Development. *Front. Cell. Neurosci.* **15**, 804649 (2022).

57. Astudillo, P. Extracellular matrix stiffness and Wnt/β-catenin signaling in physiology and disease. *Biochem. Soc. Trans.* **48**, 1187–1198 (2020).
58. Hastings, J. F., Skhinas, J. N., Fey, D., Croucher, D. R. & Cox, T. R. The extracellular matrix as a key regulator of intracellular signalling networks. *Br. J. Pharmacol.* **176**, 82–92 (2019).
59. Yang, J. et al. Unphosphorylated STAT3 accumulates in response to IL-6 and activates transcription by binding to NFkappaB. *Genes Dev.* **21**, 1396–1408 (2007).
60. Nakashima, K. et al. Synergistic signaling in fetal brain by STAT3-Smad1 complex bridged by p300. *Science* **284**, 479–482 (1999).
61. Martynoga, B., Drechsel, D. & Guillemot, F. Molecular Control of Neurogenesis: A View from the mammalian cerebral cortex. *Cold Spring Harb Perspect. Biol.* **4**, a008359 (2012).
62. Cao, F., Hata, R., Zhu, P., Nakashiro, K. & Sakanaka, M. Conditional deletion of Stat3 promotes neurogenesis and inhibits astrogliogenesis in neural stem cells. *Biochem. Biophys. Res. Commun.* **394**, 843–847 (2010).
63. Couillard-Despres, S. et al. Doublecortin expression levels in adult brain reflect neurogenesis. *Eur. J. Neurosci.* **21**, 1–14 (2005).
64. Koizumi, H. et al. Doublecortin maintains bipolar shape and nuclear translocation during migration in the adult forebrain. *Nat. Neurosci.* **9**, 779–786 (2006).
65. Hwang, I. K. et al. Age-related differentiation in newly generated DCX immunoreactive neurons in the subgranular zone of the gerbil dentate gyrus. *Neurochem Res.* **33**, 867–872 (2008).
66. Shu, T. et al. Doublecortin-like kinase controls neurogenesis by regulating mitotic spindles and M phase progression. *Neuron* **49**, 25–39 (2006).
67. Miller, F. D. & Gauthier, A. S. Timing is everything: making neurons versus glia in the developing cortex. *Neuron* **54**, 357–369 (2007).
68. Namihira, M. et al. Committed neuronal precursors confer astrocytic potential on residual neural precursor cells. *Dev. Cell.* **16**, 245–255 (2009).
69. Tchieu, J. et al. NFIA is a gliogenic switch enabling rapid derivation of functional human astrocytes from pluripotent stem cells. *Nat. Biotechnol.* **37**, 267–275 (2019).
70. Piper, M. et al. NFIA controls telencephalic progenitor cell differentiation through repression of the Notch Effector Hes1. *J. Neurosci.* **30**, 9127–9139 (2010).

Author contributions

T.H. Writing – review & editing, Writing – original draft, Methodology, Formal analysis, Experimental studies, Data curation, Conceptualization, Cell culture. S.F. Writing – review & editing. P.S.C. Writing – review & editing, Methodology. K.H.L. Writing – review & editing, Project administration, Methodology, Funding acquisition, Data curation, Conceptualization. All authors have read and approved the published version of the manuscript.

Funding

This study was funded by the Ministry of Higher Education, Malaysia, Fundamental Research Grant Scheme (FRGS/1/2022/SKK10/UPM/02/4) awarded to KHL.

Declarations

Competing interests

The authors declare no competing interests.

Additional information

Supplementary Information The online version contains supplementary material available at https://doi.org/10.1038/s41598-025-87314-y.

Correspondence and requests for materials should be addressed to K.-H.L.